Polymer 49 (2008) 5119–5127

Contents lists available at ScienceDirect

Polymer

journal homepage: www.elsevier.com/locate/polymer

Toughening epoxies with halloysite nanotubes

Shiqiang Deng [a], Jianing Zhang [a], Lin Ye [a,b,*], Jingshen Wu [c]

[a] Centre for Advanced Materials Technology, School of Aerospace, Mechanical and Mechatronic Engineering, The University of Sydney, NSW 2006, Australia
[b] Department of Mechanical Engineering, The Hong Kong Polytechnic University, Hong Kong, China
[c] Department of Mechanical Engineering, The Hong Kong University of Science and Technology (HKUST), Hong Kong, China

ARTICLE INFO

Article history:
Received 18 August 2008
Received in revised form 5 September 2008
Accepted 9 September 2008
Available online 27 September 2008

Keywords:
Nanocomposites
Halloysite
Nanotubes

ABSTRACT

An experimental attempt was made to characterize the fracture behaviour of epoxies modified by halloysite nanotubes and to investigate toughening mechanisms with nanoparticles other than carbon nanotubes (CNTs) and montmorillonite particles (MMTs). Halloysite–epoxy nanocomposites were prepared by mixing epoxy resin with halloysite particles (5 wt% and 10 wt%, respectively). It was found that halloysite nanoparticles, mainly nanotubes, are effective additives in increasing the fracture toughness of epoxy resins without sacrificing other properties such as strength, modulus and glass transition temperature. Indeed, there were also noticeable enhancements in strength and modulus for halloysite–epoxy nanocomposites because of the reinforcing effect of the halloysite nanotubes due to their large aspect ratios. Fracture toughness of the halloysite particle modified epoxies was markedly increased with the greatest improvement up to 50% in K_{IC} and 127% in G_{IC}. Increases in fracture toughness are mainly due to mechanisms such as crack bridging, crack deflection and plastic deformation of the epoxy around the halloysite particle clusters. Halloysite particle clusters can interact with cracks at the crack front, resisting the advance of the crack and resulting in an increase in fracture toughness.

1. Introduction

Epoxies are widely used nowadays in a variety of engineering applications due to their unique characteristics of high adhesive strength, relatively high strength, stiffness and hardness, and excellent chemical and heat resistance. However, most cured epoxy systems show low fracture toughness, poor resistance to crack initiation and propagation, and inferior impact strength. For example, delamination and poor impact resistance of fibre-reinforced epoxy composites are often attributed to the low fracture toughness of the epoxy matrix. Many attempts have been made in the past decades to improve the fracture toughness of epoxies by modifying epoxy resins with additives such as rubber, thermoplastics, and organic and inorganic particles. The incorporations of rubber, thermoplastics and the other polymer particles into epoxies can effectively increase their fracture toughness [1–3]. However, this improvement is compromised by reduction in some basic properties, such as strength, modulus and glass transition temperature (T_g) [4].

Inorganic additives, such as silica, alumina and glass particles, have been found to be promising modifiers for increasing the fracture toughness of epoxies without sacrificing their basic properties [5–9]. Particularly, the rapid advance of nanotechnology in recent years has inspired enormous research efforts in modifying epoxies with rigid nanoparticles or nanofibres to form epoxy nanocomposites, which were anticipated to have unique characteristics superior to those of the conventional polymer composites [8,10]. For example, organically modified montmorillonite particles (MMTs) have been widely investigated as candidate modifiers for enhancement of the properties of epoxies [11]. In those efforts, layered MMT particles were intercalated or exfoliated by a number of chemical and physical processing methods and then combined with epoxies to produce clay–epoxy nanocomposites. However, so far no remarkable improvement in mechanical properties has been reported for MMT–epoxy nanocomposites, particularly in terms of fracture toughness.

Some recent studies have shown that nano-sized silica particles produced by a sol–gel process can noticeably improve fracture toughness and other mechanical properties of epoxies at ambient temperature [12,13], in cryogenic conditions [14–16] and at elevated temperatures [15]. However, the improvements in fracture toughness were not so significant, compared with rubber-modified epoxy systems.

Carbon nanotubes (CNTs) or nanofibres (CNFs) have also been considered as ideal modifiers for the purpose of polymer modification due to their excellent strength, low density, nano-scale and, most importantly, large aspect ratios. Extensive research efforts have been made over the years in developing CNTs/epoxy

* Corresponding author. Department of Mechanical Engineering, The Hong Kong Polytechnic University, Hong Kong, China. Tel.: +61 2 93514798; fax: +61 2 93513760.
E-mail address: l.ye@usyd.edu.au (L. Ye).

0032-3861/$ – see front matter © 2008 Elsevier Ltd. All rights reserved.
doi:10.1016/j.polymer.2008.09.027

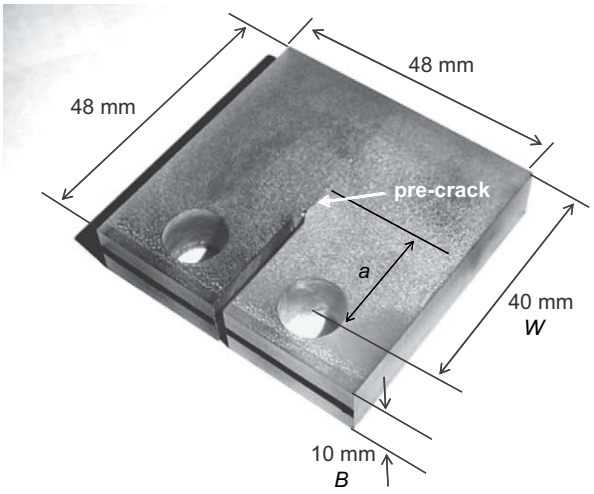

Fig. 1. Compact tension (CT) specimen for fracture toughness measurement.

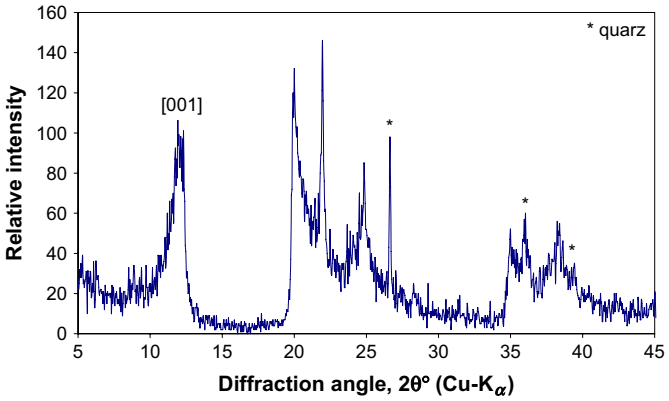

Fig. 3. XRD patterns of halloysite powders.

nanocomposites, with improved properties and performance being claimed [17–19]. However, there have been only moderate property enhancements, which are significantly below the theoretically predicted potentials [17,20]. Moreover, considering the extremely high cost and the difficulties in preparation of CNTs and CNFs, as well as their nanocomposites, developing technologies for the processing and manufacturing of nanocomposites with CNTs or CNFs in terms of quantity and cost for mass production has been one of the biggest challenges.

Recently, halloysite particles have been investigated as a new type of additive for epoxies due to their unique tubular shape [21,22], and improved properties of the resultant nanocomposites were reported, such as the coefficient of thermal expansion (CTE) and modulus [21]. More recently, Ye et al. [22] investigated epoxy nanocomposites with halloysite nanotubes. Their results demonstrated that blending epoxy with an appropriate amount of halloysite nanotubes could significantly increase impact strength without sacrificing flexural modulus, strength and thermal stability.

In contrast with other nano-sized inorganic fillers, naturally occurring halloysite nanotubes are readily obtainable and are much cheaper than other nanoparticles such as CNTs. More importantly, the unique crystal structure of halloysite nanotubes resembles that of CNTs. Therefore, halloysite particles may have the potential to provide cheap alternatives to the expensive CNTs because of their tubular structure in nano-scale and also due to their similarity to the other layered clay minerals such as MMTs, having the possibility to be further intercalated chemically or physically [23]. In the current study, an attempt is made to characterize the fracture behaviour of epoxies modified by halloysite nanoparticles, mostly nanotubes, to investigate the toughening mechanisms of such epoxy nanocomposites.

2. Experimental

2.1. Preparation of halloysite–epoxy nanocomposites

Halloysite particles (Imerys Tableware New Zealand Limited) in 5 wt% and 10 wt% were separately combined with a diglycidyl ether of bisphenol A (DGEBA) epoxy resin, Araldite-F (Ciba-Geigy, Australia), to form epoxy-based nanocomposites. The halloysite particles were first washed using acetone and then mixed with the Araldite-F epoxy by means of a mechanical mixer, stirring at 80 °C for 5 h to obtain homogeneous mixtures. After that, Piperidine hardener (Sigma–Aldrich, Australia) was added to the mixtures in a ratio of 100:5 by weight, while stirring slowly. The mixtures were then degassed in a vacuum oven (about −100 kPa) at 100 °C for about 30 min. Upon completion of degassing, the vacuum was released and the liquid mixtures were then cast into specimen cavities in preheated silicone rubber moulds and cured at 120 °C for 16 h. On the basis of designated mechanical tests, different rubber moulds were prepared to produce tensile, flexure, and compact tension specimens. Once the specimens were cooled and removed from the moulds they were milled using a surface grinder on both top and bottom surfaces to ensure flatness of specimens and, most importantly, to remove possible oversized halloysite particle aggregates, which may sink to the bottom during curing. As

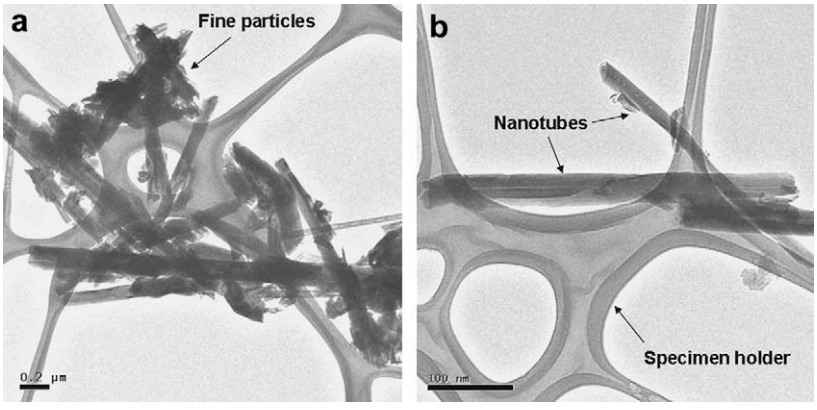

Fig. 2. TEM micrographs of halloysite particles.

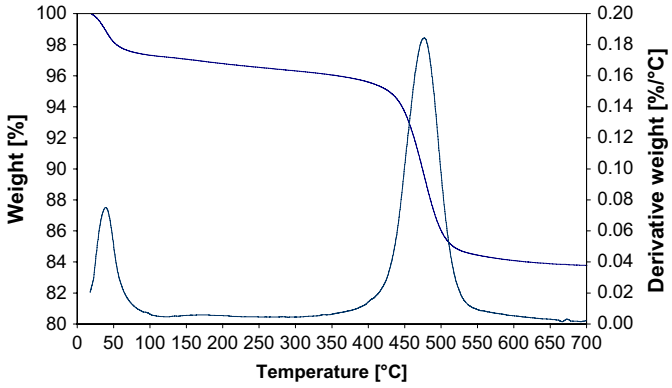

Fig. 4. Thermogravimetric curves of halloysite particles.

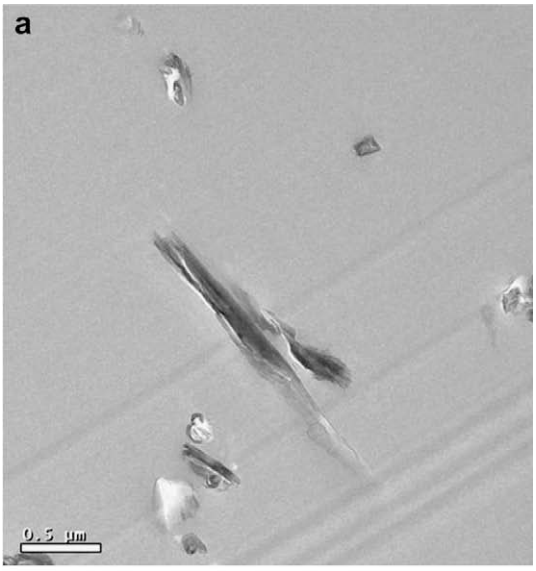

5wt% halloysite

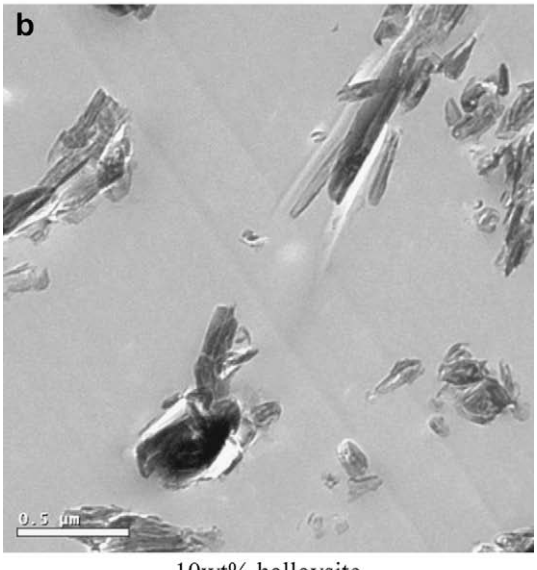

10wt% halloysite

Fig. 5. Distribution of halloysite particles in cured epoxy.

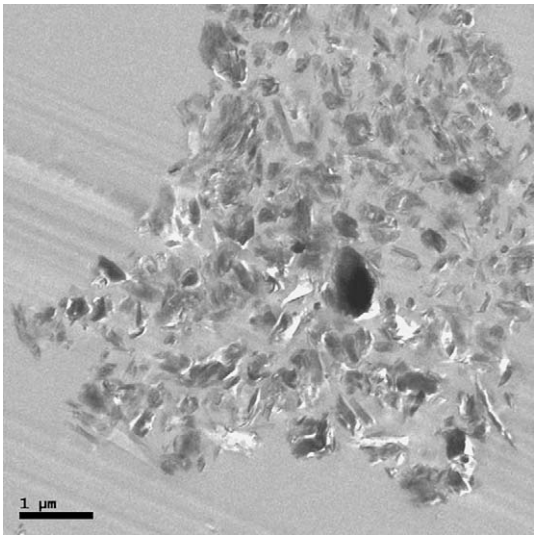

Fig. 6. Large halloysite particle cluster in cured epoxy with 10 wt% halloysite.

a baseline for comparison, specimens were also prepared for the cured neat epoxy.

2.2. Characterization of halloysite particles and halloysite–epoxy nanocomposites

Transmission electron microscopy (TEM, Philips CM120 Biofilter) and scanning electron microscopy (SEM, Philips XL30) were utilized to identify the morphology of halloysite particles, the homogeneity of halloysite particles in halloysite–epoxy nanocomposites, failure modes and toughening mechanisms. TEM specimens with a thickness of around 90 nm were prepared by thin sectioning using an ultramicrotome (Leica ultracut-S) with a diamond cutter. In particular, special TEM specimens were cut from the location where the crack tip was located, to examine the interactions between nanoparticles and the advancing crack at the crack front. SEM observations were carried out on the fracture surfaces of CT and tensile specimens after sputter coating with a thin layer of gold to increase electric conductivity.

The as-received halloysite powders were examined by X-ray diffraction analysis (XRD Siemens D5000) to characterize their crystal structure and by thermogravimetric analysis (Hi-Res TGA 2950, TA Instruments) to check their thermal stability.

The glass transition temperature (T_g) of the cured neat epoxy and the halloysite–epoxy nanocomposites were determined by

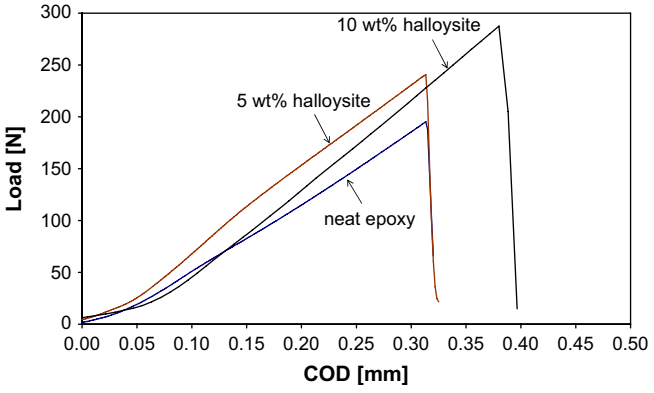

Fig. 7. Typical load *vs.* crack opening displacement (COD) curves obtained from CT tests (crack length = 19 mm).

a dynamic mechanical analyser (TA DMA 2980) with temperature scanning from ambient temperature to 150 °C at a heating rate of 3 °C/min. A three-point bending fixture was used for the DMA measurements using specimens with dimensions of 50 × 10 × 4 mm. A displacement amplitude of 20 μm was alternately applied with a frequency of 1 Hz for all DMA measurements.

2.3. Mechanical tests

The fracture toughness of the cured neat epoxy and halloysite–epoxy nanocomposites was measured using the compact tension (CT) method according to ASTM D5045. The CT specimen has a nominal dimension of 48 × 48 × 10 mm, as shown in Fig. 1. To minimize the effects of residual stress and residual plastic deformation around the crack tip, a sharp pre-crack was introduced to each CT specimen by inserting a fresh razor blade at the end of the machined crack and tapping gently with a light hammer. A loading rate of 10 mm/min was adopted, as recommended by ASTM D5045-99. As there are strict requirements for specimen geometry and crack length for accurate measurement of fracture toughness in CT tests according to the ASTM test standard, only those tested specimens which could fulfil the criteria, i.e. $a/W = 0.45$–0.55 (a is the crack length and W is the distance between the centre of the loading hole to the edge of the CT specimen, 40 mm), were used to calculate the critical stress intensity factor (K_{IC}) and critical strain energy rate (G_{IC}). At least 10 CT specimens were successfully tested for each group.

As recommended by ASTM D5045-99, K_{IC} for the compact tension specimen was calculated in two steps. First, a conditional or trial stress intensity factor (K_Q) in unites of MPa.m$^{1/2}$ was estimated by

$$K_Q = \left(\frac{P_Q}{BW^{1/2}}\right) f(x) \tag{1}$$

where $(0.2 < x = a/W < 0.8)$:

$$f(x) = \frac{(2+x)(0.886+4.64x-13.32x^2+14.72x^3-5.6x^4)}{(1-x)^{3/2}} \tag{2}$$

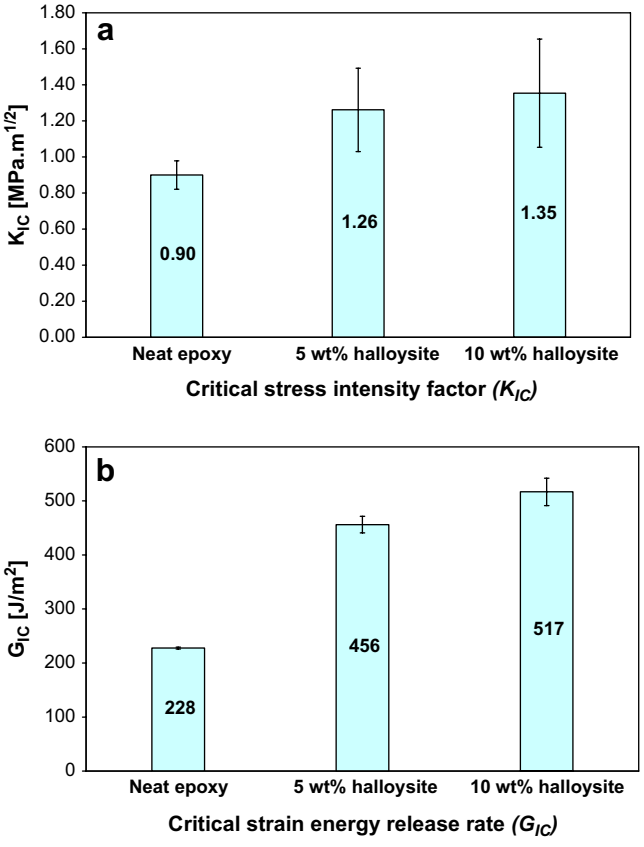

Fig. 8. Plane-strain fracture toughness of halloysite-epoxy nanocomposites.

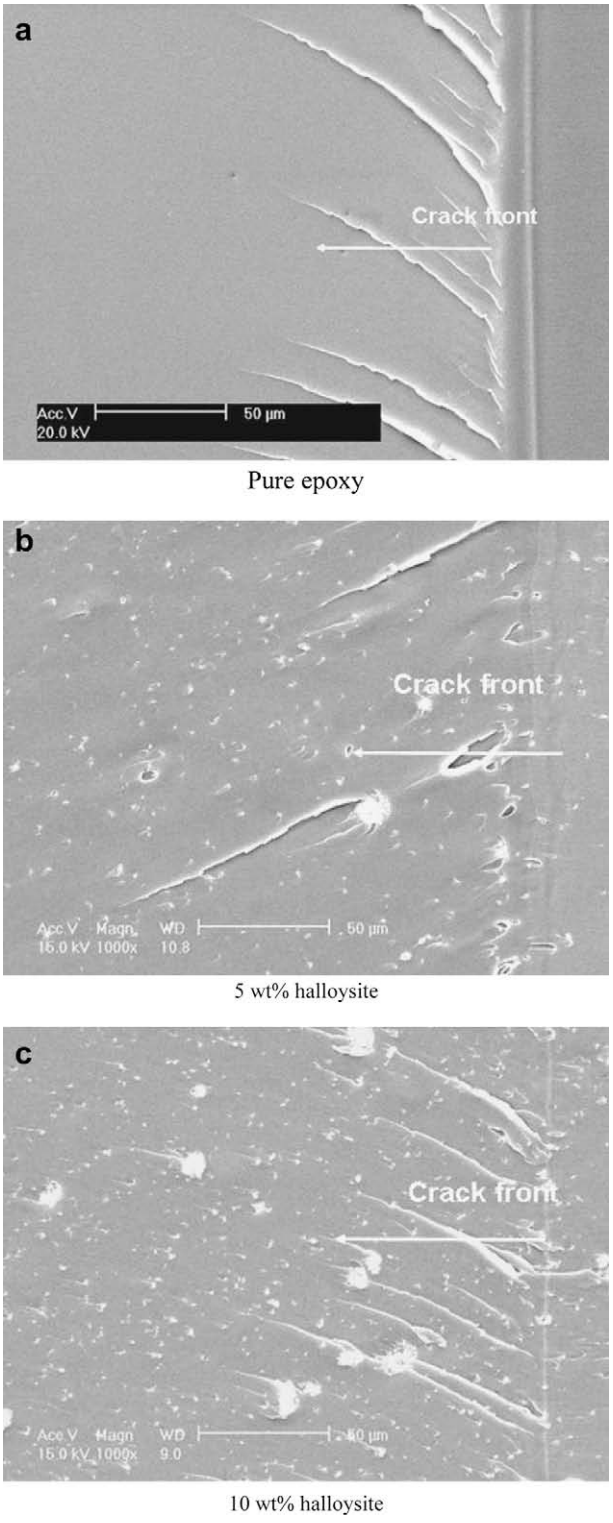

Fig. 9. SEM micrographs of fracture surfaces near crack tip, (a) pure epoxy, (b) 5 wt% halloysite, and (c) 10 wt% halloysite.

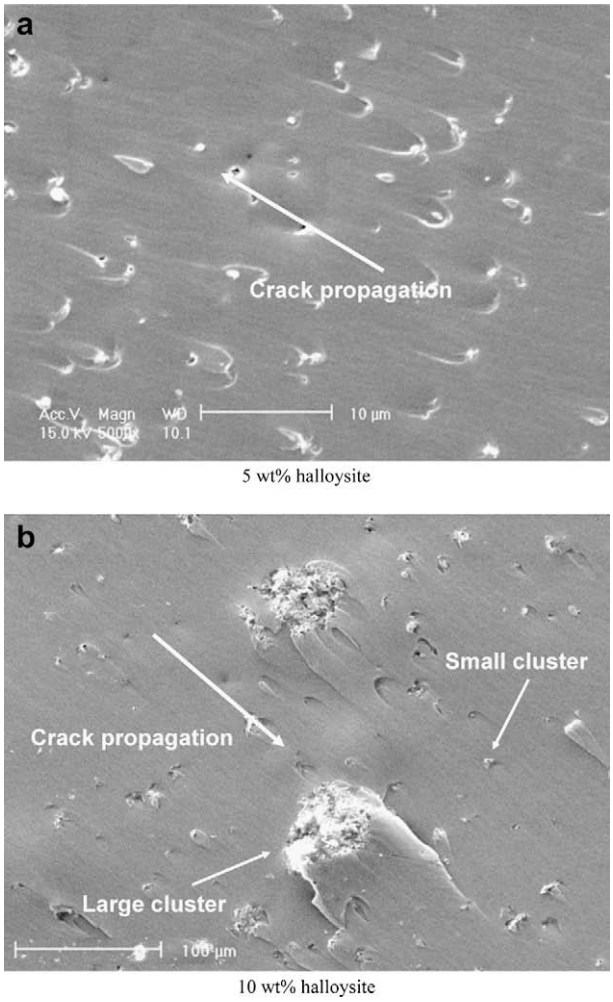

Fig. 10. Fracture surfaces of CT specimens, showing crack deflection and plastic deformation around halloysite particle clusters.

P_Q is the load determined from the load–displacement curve (a detail description for how to determine P_Q is given in the standard, and for CT specimens tested in this study, $P_Q = P_{max}$, the maximum load before failure). B is the specimen thickness.

Once K_Q is calculated, it is checked against

$$B, a, (W-a) > 2.5(K_Q/\sigma_y)^2 \tag{3}$$

where σ_y is the yield stress of the material for the temperature and loading rate of the test. If the above size criteria are satisfied for a tested CT specimen, K_Q is considered to be equal to K_{IC}, the plane strain fracture toughness. Otherwise, K_Q is not a valid K_{IC}.

In this study, G_{IC} is derived from

$$G_{IC} = \frac{\left(1-\nu^2\right)K_{IC}^2}{E} \tag{4}$$

where E is the elastic modulus of the material and ν is its Poisson's ratio. The values of σ_y, E and ν can be obtained from tensile tests.

Tension and flexure tests were also conducted to measure basic material properties of the cured neat epoxy and halloysite–epoxy nanocomposites. The tensile specimen has a dog-bone shape as required by ASTM D 638-99, with a cross-section of 13×5 mm at the gauge length region. An extensometer with a gauge length of 50 mm was attached on the surface of the tensile specimen to determine the axial strain. A loading rate of 1 mm/min was selected for all tensile tests. The flexure test specimen has a nominal dimension of $60 \times 10 \times 4$ mm. A supporting span of 48 mm and a loading rate of 3 mm/min were used for all flexural tests. At least five specimens were successfully tested for each group in the tension and flexure tests.

A universal material testing machine (Instron 5567) was used for all mechanical characterizations including tension, flexure and fracture toughness tests. All mechanical tests were conducted at ambient temperature (approximately 23 °C).

3. Results and discussion

3.1. Morphology of halloysite particles and their dispersion in nanocomposites

Halloysite is a naturally occurring aluminosilicate, $Al_2Si_2O_5(OH)_4 \cdot 2H_2O$, chemically similar to kaolinite, dickite or nacrite, differing mainly in the morphology of crystals [24]. Halloysite is a two-layered clay mineral, consisting of one alumina octahedron sheet and one silica tetrahedron sheet in a 1:1 stoichiometric ratio. Each layer bears no charge, due to the absence of isomorphic substitution in either octahedron or tetrahedron sheet. Consequently, except for water molecules, neither cations nor anions occupy the space between the layers, and the layers are held together by hydrogen bonding between hydroxyl groups in the octahedral sheets and oxygen in the tetrahedral sheets of the adjacent layers. The halloysite particle can adopt a variety of morphologies, but the most common form is an elongated hollow tubular structure with a large aspect ratio similar to that of CNTs, due to its structural defects, particularly in layer stacking of

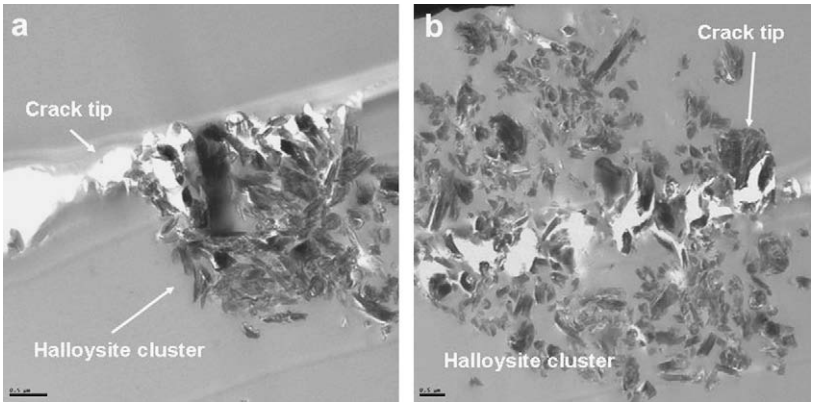

Fig. 11. TEM micrographs of halloysite-epoxy nanocomposites at crack tips.

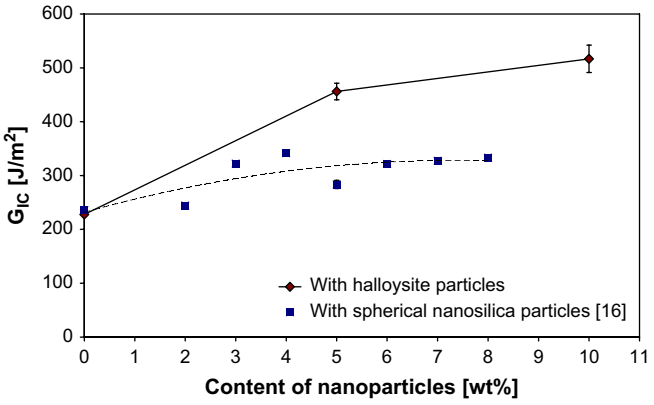

Fig. 12. Fracture toughness (G_{IC}) for epoxies modified with different nanoparticles.

the neighbouring alumina and silica layers, and their hydrated waters [24].

As shown in TEM images (Fig. 2), the halloysite particles used in this study are mainly tubular shapes with a length of 100–500 nm and a diameter of approximately 10–50 nm. There are also some other nano-sized particles of irregular form other than nanotubes, shown in Fig. 2(a).

X-ray diffraction analysis (Cu Kα) of halloysite powders was conducted and X-ray intensity patterns as a function of diffraction angle (2θ) are shown in Fig. 3. The basal spacing [001] of the halloysite particles is approximately 7.42 Å, based on the diffraction angle for the first peak ($2\theta = 11.92°$) and the wavelength of Cu Kα ($\lambda = 1.5406$ Å). In addition to halloysite, there are also minor amounts of quartz and feldspar in the powders, which was also noted by Joussein et al. [24]. The purity of halloysite particles can be further improved by certain purification processes, such as the method described in the US Patent Application (20060163160 A1).

Thermogravimetric analysis (TGA) was conducted for the as-received halloysite particles, and the results (Fig. 4) indicate that halloysite is relatively stable up to 400 °C and a weight loss of 15% occurs after the temperature exceeds 500 °C, representing the removal of the interlayer water. Note that the weight loss during the initial stage of heating prior to 50 °C was caused by the evaporation of moisture absorbed on the particle surfaces.

The dispersion of halloysite particles in the epoxy matrix is generally uniform, though most are in the form of particle clusters of different sizes, shown in Fig. 5. There are also some isolated particle clusters of relatively large size up to several microns, particularly for the nanocomposite containing 10 wt% halloysite. Although the halloysite particle clusters are not in nano-scale, they consist of numerous nano-sized particles, mainly nanotubes. The epoxy resin indeed can penetrate into the clusters, wetting these nanoparticles, which are somewhat similar to intercalated MMT particles. As shown in Fig. 6, the matrix resin has fully penetrated into a large halloysite particle cluster and formed a halloysite-rich region. This phenomenon was also identified by Ye et al. [22]. Some white areas within the halloysite cluster, shown in Fig. 6, are voids caused by TEM specimen cutting.

The dispersion of halloysite particles in the epoxy matrix is still not sufficiently homogeneous in nano-scale, because of the presence of halloysite particle clusters, in spite of the fact that the halloysite nanoparticles in the clusters are fully surrounded by the matrix resin. Most importantly, if the halloysite clusters are oversized they tend to sink to the bottom, leading to significant cross-thickness inhomogeneity which may cause a significant deterioration in mechanical properties, particularly strength and failure strain. Therefore, improvements in mixing methods, as well as modifications of particle surfaces such as by chemical treatments and ball milling, are expected to produce more homogeneous nanocomposites with reduced cluster sizes and improved halloysite–epoxy interfacial adhesion. Such nanocomposites are anticipated to have better mechanical properties than those in the current study.

3.2. Fracture toughness

Fig. 7 shows a set of typical load–crack opening displacement (COD) curves obtained from CT tests for the cured neat epoxy and halloysite–epoxy nanocomposites with halloysite content of 5 wt% and 10 wt% (crack length = 19 mm). It can be seen that both pure and modified epoxies undergo unstable crack propagation when the maximum load is reached, but the maximum load for the modified epoxies is clearly higher than that for the unmodified counterpart when the crack length of the specimens is the same. Values of the critical stress intensity factor (K_{IC}) obtained at ambient temperature are shown in Fig. 8. The magnitudes of K_{IC} of the modified epoxies were significantly improved after halloysite nanoparticles were incorporated (for both 5 wt% and 10 wt%). For the modified epoxy with 5 wt% halloysite, K_{IC} was increased up to 39% from 0.90 MPa.m$^{1/2}$ (pure) to 1.26 MPa.m$^{1/2}$, whereas for the modified epoxy with 10 wt% halloysite there was a more apparent increase in K_{IC}, up to 1.35 MPa.m$^{1/2}$, approximately 50% higher than that of the cured neat epoxy. After converting K_{IC} to G_{IC} using the equation for the plane strain condition recommended in ASTM D5045, the increases in the critical strain energy release rate (G_{IC}) were 100% and 127%, respectively, for the two halloysite–epoxy nanocomposites.

For rigid inorganic particle-filled epoxies several toughening mechanisms have been proposed, including: (a) an increase in fracture surface area due to crack deflection and crack twisting around particles; (b) enhanced plastic deformation of the epoxy

Table 1
Comparison of improvements in fracture toughness (K_{IC}) for various epoxy-based nanocomposites

Materials	Highest K_{IC} reported (MPa.m$^{1/2}$)	Improvement (%)	Comments and Ref.
Epoxy/DWCNT-NH_2 (0.5 wt%)	0.93 (measured by CT)	43 (matrix $K_{IC} = 0.65$ MPa.m$^{1/2}$)	DWCNT-NH_2 (amino-functionalized double-walled carbon nanotube) [17]
Epoxy/MWCNT (1 wt%)	6.2 (measured by SENB)	170 (matrix $K_{IC} = 2.3$ MPa.m$^{1/2}$)	MWCNT (multi-walled carbon nanotube) [25]
Epoxy/OLS (4 wt%)	2.7 (measured by SENB)	17 (matrix $K_{IC} = 2.3$ MPa.m$^{1/2}$)	OLS (Organically modified layered silicate) [25]
Epoxy/clay (5 wt%)	1.4 (measured by CT)	56 (matrix $K_{IC} = 0.9$ MPa.m$^{1/2}$)	Clay (surface modified MMTs) [26]
Epoxy/clay (10 wt%)	1.13 (measured by SENB)	53 (matrix $K_{IC} = 0.74$ MPa.m$^{1/2}$)	Clay (functionalized organosilicate) [27]
Epoxy/MMT-CPC (5 wt%)	0.99 (measured by SENB)	65 (matrix $K_{IC} = 0.60$ MPa.m$^{1/2}$)	MMT-CPC (cetylpyridinium choride treated MMT) [28]
Epoxy/clay (2.5 wt%)	1.26 (measured by SENB)	80 (matrix $K_{IC} = 0.70$ MPa.m$^{1/2}$)	Clay (methyl dihydrogenated tallow ammonium MMT) [29]
Epoxy/clay (6 wt%)	2.7 (ASTM E399-90)	−20 (matrix $K_{IC} = 3.4$ MPa.m$^{1/2}$)	Clay (surface modified MMT) [30]
Epoxy/nanosilica (8 wt%)	1.14 (measured by CT)	27 (matrix $K_{IC} = 0.90$ MPa.m$^{1/2}$)	Uniform dispersion of spherical particles with average size of ~20 nm [16]
Epoxy/nanosilica (20.2 wt%)	1.42 (ISO-13586)	141 (matrix $K_{IC} = 0.59$ MPa.m$^{1/2}$)	Uniform dispersion of spherical particles with average size of ~20 nm [31]
Epoxy/nanosilica (10.3 wt%)	0.61 (measured by CT)	45 (matrix $K_{IC} = 0.42$ MPa.m$^{1/2}$)	Uniform dispersion of spherical particles with average size of ~20 nm [32]
Epoxy/halloysite (10 wt%)	1.35 (measured by CT)	50 (matrix $K_{IC} = 0.90$ MPa.m$^{1/2}$)	Nanotubes, mostly in clusters, unmodified (current study)

CT: compact tension; SENB: single-edge-notch bending.

Table 2
Mechanical properties of halloysite nanotube modified epoxies at room temperature

Halloysite (wt%)	Tension				Flexure		
	Modulus [GPa]	Strength [MPa]	Poisson's ratio	Strain at peak load (%)	Modulus [GPa]	Strength [MPa]	Strain at peak load (%)
0	2.90 ± 0.12	62.6 ± 0.6	0.42 ± 0.03	4.49 ± 0.12	3.05 ± 0.04	111.0 ± 2.5	5.25 ± 0.03
5	2.93 ± 0.09	67.3 ± 2.0	0.40 ± 0.03	4.10 ± 0.54	3.39 ± 0.06	116.0 ± 4.5	5.16 ± 0.49
10	2.98 ± 0.10	67.4 ± 1.9	0.40 ± 0.01	4.11 ± 0.44	3.59 ± 0.08	120.3 ± 1.7	5.41 ± 0.05

around particles; and (c) crack front pinning by rigid particles [2]. For nanocomposites, if the aspect ratios of the reinforcing particles are very small, the first two mechanisms may not be very effective because of the nano-scale dimensions. However, for nanocomposites reinforced with nanotubes, such as the halloysite nanotubes, crack front pinning, or bridging, should be effective mechanisms due to the large aspect ratios. On the other hand, the halloysite–epoxy nanocomposites prepared in the current study contain many particle clusters in addition to individual particles. These particle clusters would resemble micro-sized rigid inorganic particles when confronting a crack, causing crack deflection and twisting, as well as plastic deformation. As shown in Fig. 9, the fracture surfaces of CT specimens near the crack tip are clearly different between the specimens with different amounts of halloysite. In the pure epoxy, the fracture surface is flat and smooth, implying a brittle cleavage failure, but in the 5 wt% and 10 wt% halloysite-modified epoxies there are somewhat roughened fracture surfaces with fine white particles dispersed through them, as shown in Fig. 9(b) and (c). These evenly distributed particles are the halloysite particle clusters. As shown in Fig. 10, clear uneven facades and deformations can be seen around these halloysite particle clusters of different sizes. Therefore, plastic deformation of the epoxy around particle clusters and crack deflection through the clusters may be the dominant toughening mechanisms for these halloysite–epoxy nanocomposites. As shown in Fig. 11, halloysite particle clusters can interact with the crack, bridging the crack when it passes through, resisting the advance of the crack and thus resulting in an increase in fracture toughness. Of course, as mentioned already, individual halloysite particles (nanotubes) should have crack front pinning or bridging effects because of their large aspect ratios.

On the basis of the current results, it seems that the amount of halloysite particles can be further increased to achieve even better results in fracture toughness. However, the more halloysite particles there are, the more oversized particle clusters develop, which could be detrimental to the failure behaviour of the nanocomposites. Therefore, halloysite nanoparticles should be added to a certain optimum amount.

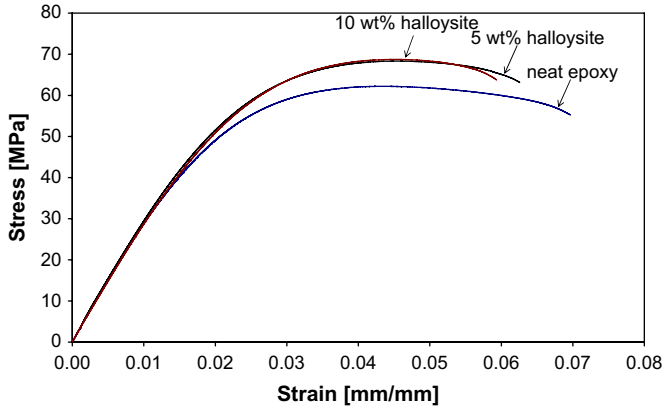

Fig. 13. Typical strain *vs.* stress curves of tensile specimens.

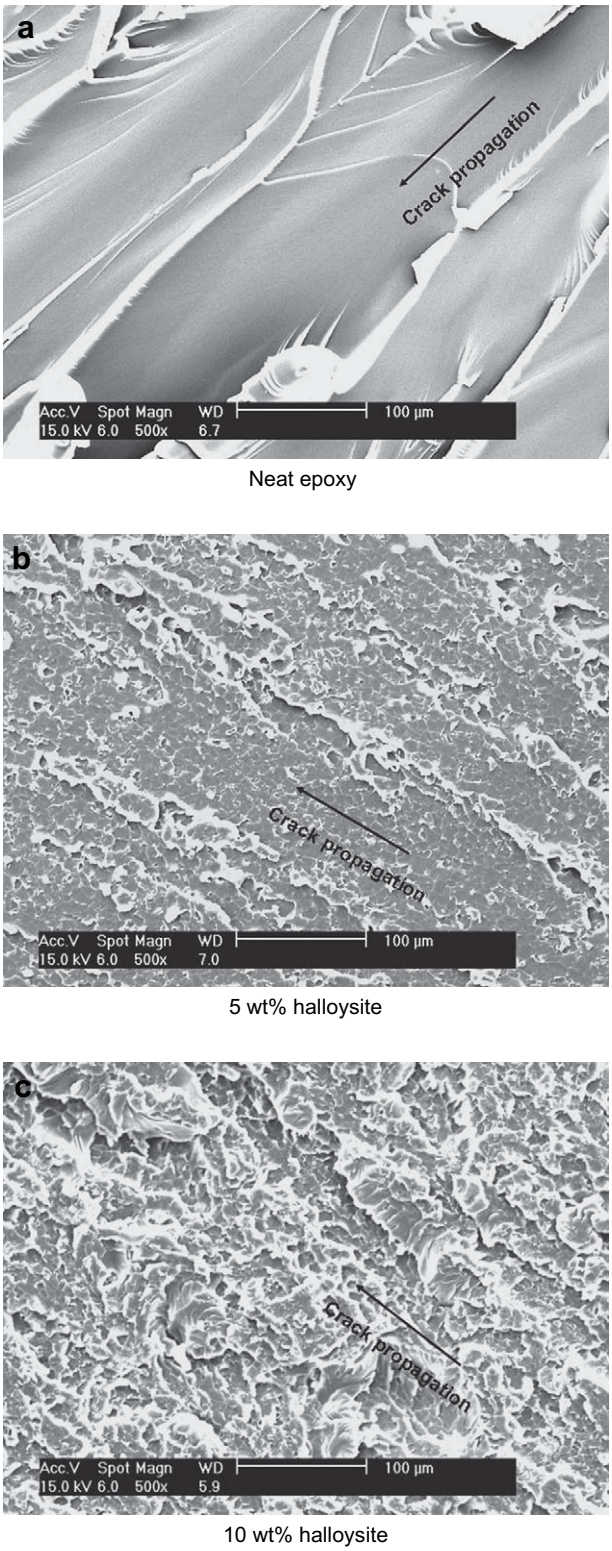

Fig. 14. SEM micrographs of fracture surfaces of tensile specimens, (a) pure epoxy, (b) 5 wt% halloysite, and (c) 10 wt% halloysite.

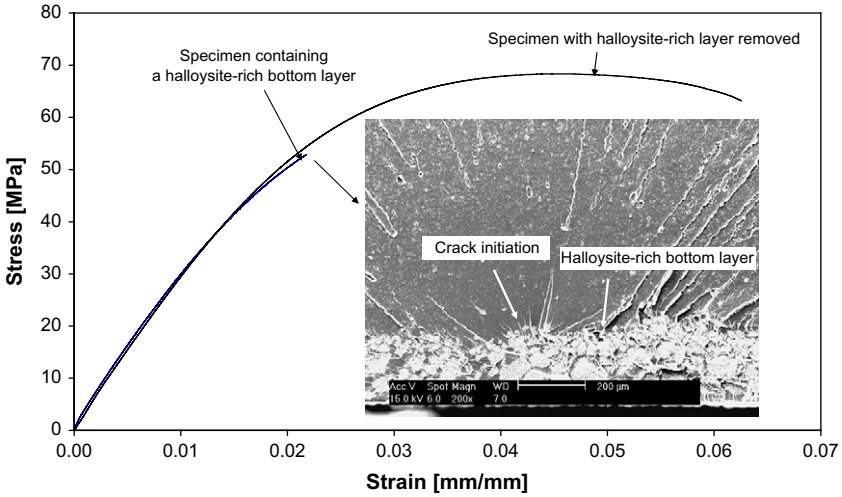

Fig. 15. Effect of oversized halloysite particle clusters on tensile failure behaviour (5 wt% halloysite).

A comparison of the fracture toughness (G_{IC}) of the same epoxy modified by halloysite and by spherical nanosilica particles is shown in Fig. 12. It can be seen that the improvement in fracture toughness of halloysite–epoxy nanocomposites is clearly greater than that of the same epoxy modified by nanosilica particles, although the nanoparticles were much more evenly dispersed in the nanosilica–epoxy nanocomposites [16] than in the halloysite–epoxy nanocomposites.

In recent years, impressive results have been published for toughening epoxies with CNTs/CNFs and MMTs. Comparison of the improvement in fracture toughness (K_{IC}) from selected sources is shown in Table 1. It can be seen that although the improvements in fracture toughness for epoxies modified by halloysite particles are not as significant as some of the reported values for epoxy–CNTs and epoxy–nanosilica (20 wt%) systems, epoxy-based nanocomposites modified with untreated halloysite particles in the current study show equivalent improvement to that of surface modified MMT–epoxy nanocomposites.

3.3. Tensile and flexural properties

Tensile and flexure properties of the cured neat epoxy and halloysite–epoxy nanocomposites are summarised in Table 2. Typical strain *vs.* stress curves of tensile specimens for three specimen groups are shown in Fig. 13. It is evident that the composites containing halloysite particles have increased strength and modulus compared to those of the cured neat epoxy. These property enhancements are attributed to the reinforcing effect of halloysite nanoparticles, especially nanotubes, as a result of their large aspect ratios. This postulation can be supported by the fracture modes of tensile specimens as shown in Fig. 14, where apparently different failure mechanisms are observed. In the cured neat epoxy, failure of the tensile specimen starts from a defect on the specimen surface or inside the specimen and undergoes substantial permanent deformation before final failure. However, for the halloysite-modified epoxies, stresses at which cracks start to grow are obviously higher because of the strengthening effect of the halloysite nanotubes, although the crack also initiates from defects somewhere on the specimen surface or within the specimen. The fracture surfaces of the tensile specimens with 5 wt% and 10 wt% halloysite particles are much rougher than that of the cured neat epoxy, showing the effect of the halloysite particles.

The toughness of a material can also be estimated by integrating the area under the tensile load–displacement curve, which is the energy consumed for breaking the sample. However, the plane strain fracture toughness of brittle materials is preferably measured by standardized tests such as CT and SENB, as recommended by ASTM D5045-99.

It is noted that oversized halloysite clusters can deposit at the bottom of the cured specimens, forming a halloysite-rich layer of about 200 μm. These oversized halloysite particle clusters in the bottom surface layer would cause premature failure of specimens under tension, with greatly reduced strength and failure strain, as shown in Fig. 15.

The removal of the halloysite-rich layer near the bottom surface would change the overall percentage of halloysite in epoxies to some extent. A rough estimation shows that the actual halloysite contents were approximately 4.5 wt% for the 5 wt% halloysite-modified epoxy, and 8.5 wt% for the 10 wt% halloysite-modified epoxy. Recently, we found that an improved mixing method with aids of ball mill homogenization and chemical treatments was able to greatly reduce cluster sizes and minimize deposition of halloysite particle clusters to the bottom, accompanied by further enhancements in mechanical performance, which will be elaborated later.

3.4. Glass transition temperatures

A summary of T_g measured by DMA using the three-point bending fixture is shown in Table 3. At least three specimens were tested for each group and the average values with standard deviations are presented. It can be seen that the addition of halloysite nanoparticles to the epoxy did not result in any significant change in T_g.

Table 3
Glass transition temperatures of halloysite-modified epoxies

Halloysite (wt%)	T_g (derived from tan δ)	
	Average	Standard deviation
0	95.5	1.9
5	96.2	1.9
10	94.7	1.1

4. Conclusions

From the experimental results obtained in this study, it can be concluded that halloysite nanoparticles, mostly in the form of nanotubes, were effective additives in increasing the fracture toughness of epoxy resins without sacrificing other properties such

as strength, modulus and glass transition temperature. The fracture toughness of the halloysite particle modified epoxies was noticeably increased, with the greatest improvement in K_{IC} up to 50% and in G_{IC} up to 127%. The improvements in fracture toughness are mainly attributable to mechanisms such as crack bridging, deflection and plastic deformation of the epoxy around the particle clusters. Halloysite particle clusters can interact with cracks at the crack front, resisting the advance of the crack and resulting in an increase in fracture toughness. In addition to the improvement in fracture toughness, there were also noticeable enhancements in strength and moduli for halloysite–epoxy nanocomposites due to the reinforcing effect of the halloysite nanotubes.

It appears that, without any treatment, halloysite nanoparticles tend to aggregate and form clusters in the epoxy matrix, even though the epoxy resin can penetrate into the clusters. Oversized clusters would impair the mechanical performance of the nanocomposites. Therefore, further improvements in particle surface modifications and in mixing methods are expected to produce more uniform nanocomposites with improved mechanical properties. Moreover, due to the unique morphology of halloysite, alignments of halloysite nanotubes in epoxies would have effects on mechanical performance of halloysite–epoxy nanocomposites, possibly in a similar manner as in CNTs-modified epoxies. Therefore, aligning halloysite nanotubes in certain preferred orientations by appropriate methods during mixing, for example shear flow, may produce halloysite–epoxy nanocomposites with anisotropic performance analogous to aligned short fibre-reinforced composites.

References

[1] Bascom WD. J Appl Polym Sci 1975;19:2545.
[2] Garg AC, Mai Y-W. Compos Sci Technol 1988;31:179.
[3] Kinloch AJ. NATO ASI Ser E Appl Sci 1985;89:393.
[4] Garg AC, Mai Y-W. Compos Sci Technol 1988;31:225.
[5] Balakrishnan S, Start PR, Raghavan D, Hudson SD. Polymer 2005;46:11255.
[6] Imanaka M, Takeuchi Y, Nakamura Y, Nishimura A, Iida T. Int J Adhes Adhes 2001;21:389.
[7] Kinloch AJ, Lee JH, Taylor AC, Sprenger S, Eger C, Egan D. J Adhes 2003;79:867.
[8] Kinloch AJ, Taylor AC. J Mater Sci Lett 2003;22(20):1439.
[9] Koh SW, Kim JK, Mai Y-W. Polymer 1993;34(16):3446.
[10] Njuguna J, Pielichowski K, Alcock JR. Adv Eng Mater 2007;9(10):835.
[11] Hussain F, Hojjati M, Okamoto M, Gorga R. J Comput Mater 2006;40(17):1511.
[12] Rosso P, Ye L, Friedrich K, Sprenger S. J Appl Polym Sci 2006;100(3):1849.
[13] Zhang K, Wang L, Wang F, Wang G, Wang G, Li Z. J Appl Polym Sci 2004;91(4):2649.
[14] Huang CJ, Fu SY, Zhang YH, Lauke B, Li LF, Ye L. Cryogenics 2005;45(6):450.
[15] Deng S, Ye L. Key Eng Mater 2006;312:243.
[16] Deng S, Ye L, Friedrich K. J Mater Sci 2007;42(8):2766.
[17] Gojny FH, Wichmann MHG, Fiedler B, Schulte K. Compos Sci Technol 2005;65:2300.
[18] Ganguli S, Bhuyan M, Allie L, Aglan H. J Mater Sci 2005;40(13):3593.
[19] Gojny FH, Wichmann MHG, Kopke U, Fiedler B, Schulte K. Compos Sci Technol 2004;64(15):2363.
[20] Maniar KK. Polym-Plastics Tech Eng 2004;43(2):427.
[21] Liu M, Guo B, Du M, Cai X, Jia D. Nanotechnology 2007;18(45):455703.
[22] Ye Y, Chen H, Wu JS, Ye L. Polymer 2007;48(21):6426.
[23] Horvath E, Kristof J, Frost RL, Redey A, Vagvolgyi V, Cseh T. J Therm Anal Calorim 2003;71(3):707.
[24] Joussein E, Petit S, Churchman J, Theng B, Righi D, Delvaux B. Clay Miner 2005;40(4):383.
[25] Ganguli S, Aglan H, Dean D. J Elasto Plastics 2005;37(1):19.
[26] Zerda AS, Lesser AJ. J Polym Sci B Polym Phys 2001;39(11):1137.
[27] Brunner AJ, Necola A, Rees M, Gasser P, Kornmann X, Thomann R, et al. Eng Fract Mech 2006;73(16):2336.
[28] Qi B, Zhang QX, Bannister M, Mai Y-W. Comput Struct 2006;75(1–4):514.
[29] Wang K, Chen L, Wu JS, Toh ML, He CB, Yee AF. Macromolecules 2005;38:788.
[30] Ha SR, Rhee KY, Kim HC, Kim JT. Colloids Surf A Physicochem Eng Aspect 2008;313-314:112.
[31] Kinloch AJ, Mohammed RD, Taylor AC, Eger C, Sprenger S, Egan D. J Mater Sci 2005;40(18):5083.
[32] Zhang H, Zhang Z, Friedrich K, Eger C. Acta Mater 2006;54:1833.